Polarization, band lineups, and stability of SiC polytypes

A. Qteish,* Volker Heine, and R. J. Needs
Cavendish Laboratory, University of Cambridge, Madingley Road, Cambridge CB3 0HE, England
(Received 16 July 1991; revised manuscript received 16 October 1991)

We calculate the spontaneous polarization of wurtzite-structure SiC, using the recently proposed supercell technique of Posternak, Baldereschi, Catellani, and Resta [Phys. Rev. Lett. **64**, 1777 (1990)] and a first-principles pseudopotential approach. The macroscopic polarization is found to be 4.32×10^{-2} C/m^2, and is mainly due to the electronic-charge-density redistribution rather than a relaxation of the positions of the ions. The valence-band offset at the interface between the wurtzite and cubic forms is determined using the same supercell calculations, giving 0.13 eV, with the wurtzite-structure SiC valence-band edge being higher in energy. Our calculations also predict the crystal-field splitting of the top of the valence band of wurtzite-structure SiC to be 0.12 eV, and give some insight into the nature of the dipole created by a single stacking fault. Finally, the effect of the macroscopic electric fields on the relative stability of SiC polytypes is discussed and found to be negligible.

I. INTRODUCTION

SiC exists in many polytypes, namely the cubic zinc-blende structure $\langle\infty\rangle$ ($3C$), wurtzite structure $\langle1\rangle$ ($2H$), and the polytypes $\langle2\rangle$ ($4H$) and $\langle3\rangle$ ($6H$), with many intermediate phases, such as $\langle23\rangle$ between the last two. These polytypes can be generated by certain patterns of stacking faults along the [111] direction of an otherwise perfect cubic structure $\langle\infty\rangle$. Apart from the $\langle\infty\rangle$ structure, other lower-symmetry polytypes are expected to possess an intrinsic spontaneous polarization (SP): since the four tetrahedral bonds are no longer equivalent bond-to-bond charge transfer and ionic relaxation[1] may cause SP along the stacking direction.

The present paper has three main purposes. Firstly, to study the SP of $\langle1\rangle$ SiC, using a quantum-mechanical approach. The interpretation of the SP is of fundamental importance in the theory of dielectrics, and is still an open problem: the localized dipoles used in the classical treatment have not been justified from quantum-mechanical calculations. Quantum-mechanical treatments of the SP in pyroelectrics have only just begun,[2] and more work is obviously needed to enhance our understanding of its origin. Secondly, to calculate the band offsets at the interfaces between SiC polytypes: the importance of their determination comes from the large variation of the band gap of SiC between different polytypes.[3] Thirdly, to investigate the effects of the SP and band offsets on the relative stability of SiC polytypes. The relative stability of these polytypes has been thoroughly studied using a first-principles approach.[1,4–8] It has been shown that the $\langle1\rangle$ structure has a significantly higher energy than the $\langle2\rangle$ and $\langle3\rangle$ polytypes and yet SiC can be crystallized in that form. Another striking feature is the existence of polytypes with very long repeat distances. We will discuss the possibility that these polytypes are stabilized by the presence of their intrinsic SP.

Our calculations were performed using a first-principles pseudopotential technique and the local-density approximation for the exchange-correlation potential. In Sec. II we describe our method and the computational details.

The SP of crystals is very difficult to determine both experimentally and theoretically. It leads to an electric potential difference between the two ends of a finite crystal, along the polarization axis. This is usually compensated by attracting charges from the air, and/or by the migration of electrons and holes due to impurities from inside the material. Furthermore, the SP of a finite slab depends on the state of the crystal surfaces, which makes the SP dependent on sample preparation and external conditions. Some quantities do not depend on the state of the crystal surfaces, such as the variation of the SP with respect to strain, temperature, or a zone-center optical phonon,[9] because these do not alter the condition of the surfaces. On the other hand, the use of Born–von Kármán boundary conditions to recover the thermodynamic limit makes the SP inaccessible to first-principles calculations performed for a unit cell of a bulk material. Very recently another approach has been proposed by Posternak, Baldereschi, Catellani, and Resta (PBCR).[2] PBCR have shown that the SP in a slab of $\langle1\rangle$ BeO, with faces normal to the polarization axis, can be determined as the difference between the SP in such a slab and in a similar slab of the $\langle\infty\rangle$ form (which has zero bulk SP, by symmetry). The two structures are perfectly matched at the (111) interface, which is a very natural boundary, indeed the only sensible one, for defining the SP. The two slabs are then infinitely repeated to allow for a quantum-mechanical treatment of the problem in a supercell geometry; see Fig. 1. PBCR have concluded that the SP in $\langle1\rangle$ of BeO is mostly due to the ionic relaxation. The work of PBCR has opened the door to first-principles studies of the macroscopic polarization of pyroelectric and ferroelectric materials. In the present paper we will focus on the SP in the $\langle1\rangle$ form of SiC which has the largest hexagonal character among the po-

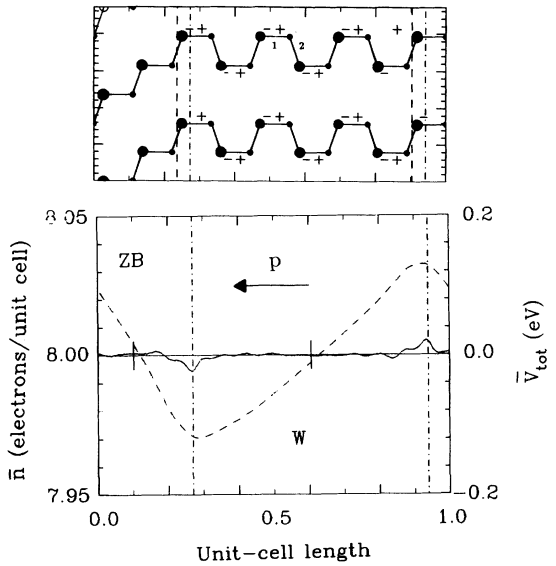

FIG. 1. Upper panel: Si-C bond chains along the stacking direction in the unrelaxed $3\langle\infty\rangle/6\langle1\rangle$ SiC superlattice used in our calculations. Small and large solid circles represent C and Si atoms, respectively. 1 and 2 refer to the bonds along which the charge density is plotted in Fig. 5. Dashed lines: the interfaces defined by Northrup, Ihm, and Cohen (Ref. 16); dashed-dotted lines: the interfaces considered in this work (see text). The + and − signs refer to the positions of the maximum pile-up of holes and electrons, respectively, as shown in Fig. 6. Lower panel: Averaged charge density (solid lines) $\bar{n}$ and averaged total potential (dashed lines) $\bar{V}_{tot}$, of the above superlattice. The halfway points between the interfaces in the $\langle\infty\rangle$ and $\langle1\rangle$ regions are indicated by short vertical solid lines. The arrow shows the direction of the SP in the $\langle1\rangle$ slab of SiC.

lytypes. The results will be discussed in connection with the valence electronic-charge-density redistribution and ionic relaxation in Sec. III, and we conclude that the SP is mostly due to the electronic-charge-density redistribution.

Interestingly, the band gap of SiC is found to increase almost linearly with the percentage of hexagonal character:[2] it varies from 2.39 eV in the $\langle\infty\rangle$ structure to 3.30 eV in the $\langle1\rangle$ form. In other materials, such as ZnS (Ref. 8) (which also exists in many polytypes) and CdS (Ref. 10) (which can be grown in the $\langle1\rangle$ and $\langle\infty\rangle$ structures), the electronic band structures of the $\langle1\rangle$ and $\langle\infty\rangle$ structures are found to be very similar and in these cases the difference in band gaps is less than 0.1 eV. Any polytype can be thought of as being made out of small units of $\langle\infty\rangle$, $\langle1\rangle$, $\langle2\rangle$, and $\langle3\rangle$, and therefore we are interested in the band offsets between these simple polytypes. Since the total-energy differences between the different polytypes are very small, the ratio between the valence- and conduction-band offsets is also expected to be very small. Very recently Heine, Cheng, and Needs[11] have used the argument of a vanishing valence-band offset (VBO) to discuss the stability of $\langle\infty\rangle$, $\langle1\rangle$, and other polytypes in the presence of donor and acceptor impurities. The most time consuming part of a calculation of the VBO is the determination of the difference in the averaged total potential in the two materials, which requires a supercell containing both materials. However, this difference can be determined easily from the same supercell calculations used to calculate the SP. In Sec. IV we present and discuss our results obtained for the VBO at the $\langle\infty\rangle/\langle1\rangle$ SiC interface, and discuss the possibility of using these results to obtain the VBO at the (111) interfaces between any other pair of SiC polytypes.

The presence of SP and the consequent electric fields in SiC have not been considered before in relation to the relative structural stability of different polytypes. A polytype may be considered as a particular stacking of atomic double layers (hereafter referred to as layers) in what would be the [111] direction of the cubic zinc-blende structure. Each layer can be placed on top of the one below on one of two different ways, to which we can assign a plus sign and a minus sign, respectively. An arbitrary polytype can be considered as a band of n_1 layers stacked as in a cubic crystal, to which we assign a plus sign, followed by an antiphase boundary and n_2 layers stacked in the minus sense,[7,8] and so on. Since there can be no SP in cubic zinc-blende-structure materials, we may associate the SP with the antiphase boundaries. The point is that there are substantial electric fields and voltage variations set up in real polytypes analogous to our very artificial supercell structure in Fig. 1. Two questions arise. First, the computations of the relative energies of various polytypes reported in Refs. 1 and 4–8 used periodic boundary conditions in the normal way. Such periodic boundary conditions are usually considered a convenient mathematical device devoid of physical reality, and one may wonder whether their use incorporates correctly the electrostatic effects associated with a real crystal. We shall consider this issue in Sec. V and conclude that the periodic boundary conditions are in fact appropriate for bulk structural energies. Second, we see from Fig. 1 that in a polytype with a long repeat distance there will be a substantial potential variation. In real SiC materials at the temperatures of crystal growth there will be mobile free electrons and/or holes which can flow from regions of high to regions of low potential energy, and thus lower the total energy of the system. The potential variation would be screened out by such free-carrier motion, and one wonders whether the effect can give a long-range interaction to stabilize long-period polytypes, in addition to the mechanisms already considered previously.[1,4–8] This will be also discussed in Sec. V, and again we shall conclude that there is nothing in it. Finally, a summary of our main results and conclusions will be given in Sec. VI.

II. METHOD AND COMPUTATIONAL DETAILS

The macroscopic polarization of an electronic-charge-density distribution in a crystal, $n(\mathbf{r})$, is by definition the electric dipole moment per unit volume,

$$P=\frac{1}{v}\int d\mathbf{r}\cdot\mathbf{r}n(\mathbf{r})\ . \tag{1}$$

Modern first-principles techniques are capable of determining $n(\mathbf{r})$ with very high accuracy, as has already been

done for many materials. One might therefore think that P could be determined easily using Eq. (1). Unfortunately, this is not the case: for an infinite crystal without a center of inversion the polarization obtained according to Eq. (1) is an ill-defined quantity.[12] For a finite piece of material, P is well defined but it depends crucially on the truncation at the surfaces. In addition, surface-induced effects, caused by surface reconstruction and the accumulation of extra charges, can affect P.

In order to eliminate the truncation and surface effects, PBCR proposed that the polarization in a finite slab of the polarized material, with faces normal to the polarization axis, can be obtained as the difference in the polarization ΔP in this slab and in a similar slab of an arbitrary reference material, which has no bulk SP by symmetry, and which is perfectly matched to the polarized slab normal to the polarization axis in order to eliminate any chemical (e.g., broken bonds, ionic or electronic charge transfer) or geometrical (e.g., reconstruction) effects. The ideal reference material for the $\langle 1 \rangle$ and other polytype structures is the cubic $\langle \infty \rangle$ form of the same material with lattice parameter equal to that of the polarized structure normal to the stacking direction as shown in Fig. 1. ΔP can then be calculated by performing first-principles calculations for a supercell which has the above two slabs (the polarized and the reference) as the basic building block. PBCR found that ΔP converged very rapidly with respect to the size of the unit cell.

The $\langle 1 \rangle$ structure has three independent structural parameters, which we take as the lattice parameter a normal to the stacking direction, the c/a ratio where c is the lattice parameter along the stacking direction, and the internal relaxation parameter u defined as d_L/c with d_L is the length of the longitudinal (L) bond along the stacking direction. The ideal values of c/a and u are 1.633 and 0.3750, respectively. The equilibrium parameters for the $\langle 1 \rangle$ form of SiC have been calculated using a first-principles pseudopotential technique by Cheng, Needs, and Heine,[1] giving values for c/a and u of 1.640 and 0.3755, respectively.

Following PBCR we have used a supercell approach to calculate from first-principles the SP in the $\langle 1 \rangle$ structure of SiC. The unit cell from which the results reported in Sec. III were extracted is shown in Fig. 1. As a consequence of the SP in the $\langle 1 \rangle$ region and the depolarization field (which results from the use of periodic boundary conditions), the averaged potential along the polarization axis is expected to show a sawtoothlike shape. However, in reality, because of the finite width of the interface, the averaged potential at the edges becomes smooth as shown in Fig. 1. The averaged potential from which ΔP can be extracted will be discussed below. The averaging was performed using the moving-slab averaging method of Baldereschi, Baroni, and Resta.[13] The integration limits along the polarization axis for the slab averaging were $-c/4$ and $c/4$ from the point under consideration.

The calculation of ΔP was done first with the Si and C atoms occupying the ideal tetrahedral atomic positions (hereafter referred to as the unrelaxed configuration), and then we relaxed the structure such that the $\langle 1 \rangle$ slab had the calculated equilibrium values of c/a and u,[1] see above (hereafter referred to as the relaxed configuration). For the unrelaxed configuration the sum of the averaged ionic ($\bar{V}_{\rm ion}$) and exchange-correlation potentials ($\bar{V}_{\rm EC}$) is equal to a constant (assuming a sharp interface and a constant averaged charge density in the two regions) or a very weakly varying function of z along the stacking direction, as found in the real calculations. In the unrelaxed case, ΔP can therefore be extracted from the averaged Hartree potential ($\bar{V}_H$). Whereas in the relaxed configuration ΔP must be extracted from $\bar{V}_{\rm ion}+\bar{V}_H$. In practice $\bar{V}_{\rm EC}$ is found to be a sufficiently weakly varying function of z that in both cases one can use the averaged total potential

$$\bar{V}_{\rm tot}=\bar{V}_{\rm ion}+\bar{V}_H+\bar{V}_{\rm EC} , \tag{2}$$

including the exchange-correlation term. This is convenient because $\bar{V}_{\rm tot}$ is also the quantity we use in the calculations of the band offsets. Therefore, ΔP is extracted for both the relaxed and unrelaxed configurations from $\bar{V}_{\rm tot}$ using the relation (in SI units)

$$\Delta P=-\epsilon_0\,\Delta E=-\epsilon_0\left[\frac{\partial \bar{V}_{\rm tot}(W)}{\partial z}-\frac{\partial \bar{V}_{\rm tot}(C)}{\partial z}\right] , \tag{3}$$

where W and C refer to the wurtzite and cubic regions of the supercell. In this way what we are really calculating is the difference in the polarizations, ΔP, between the two slabs included in the supercell. By increasing the width of the slabs until ΔP is well converged, ΔP can then be associated with the difference in the polarizations of the two bulk materials, which gives directly the SP in the $\langle 1 \rangle$ structure.

The SP calculated in this manner is the polarization one would measure in a thick slab of the $\langle 1 \rangle$ structure sandwiched between two semi-infinite crystals of the cubic structure $\langle \infty \rangle$ of the same material. This polarization is independent of the thickness of the $\langle 1 \rangle$ slab, provided that it is reasonably thick. Therefore, the calculated SP corresponds to that of a finite piece of the $\langle 1 \rangle$ structure after eliminating, in a *particular way,* the truncation and surface-induced effects. One should stress again that the calculated SP is not the intrinsic SP, $P_{\rm int}$, of the $\langle 1 \rangle$ (the so-called transverse SP in Ref. 2), but it is the sum of the intrinsic and induced SP's. It is not difficult to write down and solve the classical macroscopic equations of electrostatics for our geometry, including the induced polarizations due to the electric fields present in the $\langle 1 \rangle$ and $\langle \infty \rangle$ regions. We obtain

$$P_{\rm int}=\epsilon_\infty\,\Delta P , \tag{4}$$

where ϵ_∞ is the dielectric constant (assumed the same for the $\langle 1 \rangle$ and $\langle \infty \rangle$ materials) equal to 6.52 for SiC.[14]

Another way of extracting ΔP is by calculating the net pile-up of charge σ at the interfaces between the two structures, and using the relation

$$\Delta P=-\sigma . \tag{5}$$

However, the first method is much easier, since σ is very small compared with the total valence charge density, as one can see from Fig. 1.

Details of the method of calculating VBO's are described in Ref. 15. In the present case the VBO is the sum of two terms: (i) the difference between $\bar{V}_{\rm tot}$ in the two structures (the so-called potential lineup), and (ii) the difference in the energy of the top of the valence band calculated relative to a constant averaged total potential ($\bar{V}_{\rm tot}=0$) in each of the two structures. Contributions from spin-orbit splitting and the many-body corrections to the local-density approximation are expected to be negligible in the present case, because they are very similar in the two structures. The PBCR approach to calculate the SP is completely analogous to the method usually used to calculate the potential lineup. In fact, both quantities can be obtained from a single supercell calculation. If the potential lineup is zero, then $\bar{V}_{\rm tot}$ changes sign at the halfway points between the two interfaces in each of the two regions, and is expected to have a maximum or minimum at the interface. If the potential lineup is not zero, then $\bar{V}_{\rm tot}$ will not change sign precisely at the halfway points, and the potential lineup is then equal to the difference in the values of $\bar{V}_{\rm tot}$ at the halfway points, or equivalently to the discontinuity at the interface obtained by linearly extrapolating $\bar{V}_{\rm tot}$ around the halfway points (as would be the case if there were no interface smoothing resulting from the finite width of the interface), as shown schematically in Fig. 2. The second contribution to the VBO can be obtained from separate calculations for the two bulk structures.

For an accurate determination of the VBO a sharp interface must be unambiguously defined. Using the argument that the Si and C atoms on opposite sides of the interface are affected by the change in the structure at the level of the fourth-nearest neighbors in the other structure, Northrup, Ihm, and Cohen[16] have defined a sharp interface between the $\langle 1 \rangle$ and $\langle \infty \rangle$ structures of the same material shown by vertical dashed lines in Figs. 1 and 3. However, this definition seems to be inconsistent with the electric dipole crated by a single stacking fault,[17] which is found to be across the T bond and not across the central L bond as one would expect from the Northrup,

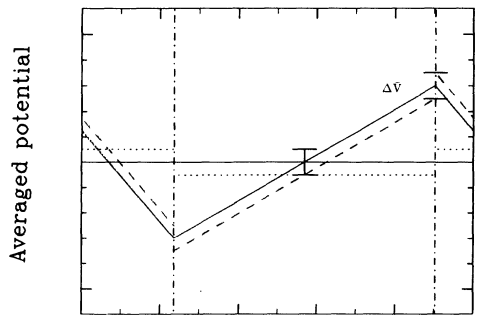

FIG. 2. Averaged electrostatic potential with zero (solid line) and finite (dashed line) potential lineup $\Delta\bar{V}$ (schematic), see text. The averaged electrostatic potential assuming zero SP is shown by dotted lines, and the interfaces are shown by vertical dashed-dotted lines.

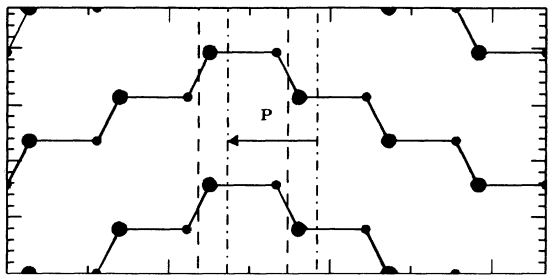

FIG. 3. Interfaces between an isolated antiphase boundary and its surrounding cubic regions. Dashed vertical lines represent the interfaces of Northrup, Ihm, and Cohen (Ref. 16); the dashed-dotted lines are the interfaces defined in present work (see also Fig. 1). The arrow indicates the direction and location of the expected electric dipole.

Ihm, and Cohen[16] interfaces between the stacking fault and the surrounding cubic regions (see Fig. 3). One can also argue that the interface should be at the middle of the L bond, since the polytype structure is determined by the direction of its T bonds. From our calculations we have found that the second choice is more physical but the interface is closer to the Si end of the interface L bonds than to the C end (see Sec. III).

Our calculations were performed using the self-consistent pseudopotential technique and the local-density approximation[18] for the exchange-correlation potential. For the exchange-correlation potential we used the Ceperley-Alder[19] form as parametrized by Perdew and Zunger.[20] For the Si and C pseudopotentials we have taken those previously used in the SiC calculations.[1,4-8] In the supercell calculations, the wave functions were expanded in a plane-wave basis set including all waves up to 20 Ry in energy, while in the bulk $\langle \infty \rangle$ (six atoms per unit cell) and $\langle 1 \rangle$ (four atoms per unit cell) a 32-Ry cutoff was used. The effect of these cutoffs was checked by increasing them to 32 and 45 Ry, respectively, and they were found to have negligible effects on both the SP and the VBO (less than 1%). The Brillouin-zone integrations were performed by sampling on regular $4\times4\times2$, $4\times4\times6$, and $4\times4\times4$ Monkhorst-Pack[21] meshes for the supercell, $\langle 1 \rangle$ and $\langle \infty \rangle$, structures, respectively. The last two meshes were chosen such that the same set of special points is used for the two bulk structures.[5] We increased the size of the supercell until the averaged charge density converged to its bulk value and until $\bar{V}_{\rm tot}$ became a linearly varying function with respect to the distance around the halfway points. We found that three layers of $\langle \infty \rangle$ and six of $\langle 1 \rangle$ in the supercell were enough for excellent convergence, as can be seen from Fig. 1.

III. RESULTS FOR THE SPONTANEOUS POLARIZATION AND VALENCE CHARGE DENSITY

The averaged valence charge density $\bar{n}$ and averaged total potential $\bar{V}_{\rm tot}$ along the polarization direction for the unrelaxed superlattice structure are also shown in Fig. 1. The important features to note are (i) the

sawtoothlike shape of $\bar{V}_{tot}$, which indicates the presence of SP in the $\langle 1 \rangle$ structure; (ii) the sharp interfaces postulated from simple arguments[16] do not coincide with the location of the maxima and minima of $\bar{V}_{tot}$ at the interface region: the latter seem to be shifted by about one T-bond distance along the stacking direction; (iii) $\bar{V}_{tot}$ does not change sign at the halfway points between the two interfaces, which shows that $\bar{V}_{tot}$ is not identical in the bulk $\langle \infty \rangle$ and $\langle 1 \rangle$ forms (in the absence of the polarization).

The calculated intrinsic SP, P_{int} in $\langle 1 \rangle$ SiC according to Eqs. (3) and (5) and Fig. 1 is 3.33×10^{-2} C/m^2. This value is larger than the value (1.57×10^{-2} C/m^2) obtained by PBCR for the unrelaxed $\langle 1 \rangle$ BeO (Ref. 2) using the self-consistent full-potential linearized augmented-plane-wave method. This is mainly due to the large difference in the values of the dielectric constants of BeO (2.99) and SiC (6.52). Since the ionic relaxation is not yet included, this SP is due only to the electronic-charge-density redistribution, resulting from the introduction of the stacking faults required to transform the cubic $\langle \infty \rangle$ structure into the $\langle 1 \rangle$ form. In Fig. 4 we show a contour plot of the valence charge density along the bond chain of our SiC supercell structure. Figure 4 shows that the charge densities along the L and the T bonds in the $\langle 1 \rangle$ region are very similar and, in turn, are similar to those in the $\langle \infty \rangle$ region, which demonstrates that the charge density redistribution is really very small. To highlight this feature we show in Fig. 5 the charge density along the L and T bonds and the difference between them. From Fig. 5 it appears that the L bond has on average a higher charge density, contrary to what one expects from the relaxation of $\langle 1 \rangle$ SiC.[1] Total energy and force calculations[1] have shown that the T bond is shorter than the L one, suggesting that there is a flow of electrons from the L to the T bonds on going from $\langle \infty \rangle$ to $\langle 1 \rangle$. In order to get more insight into the electronic charge transfer and to show that there really is a transfer of electrons from the L to the T bonds, we show in Fig. 6 the difference between the charge densities of the bulk $\langle 1 \rangle$ and $\langle \infty \rangle$ forms averaged in the planes normal to the stacking direction. The important features to note are (1) in the T-bond regions there is an excess of charge in agreement with the relaxation of the $\langle 1 \rangle$ form; (2) most of the charge transfer takes place in the L-bond region or across

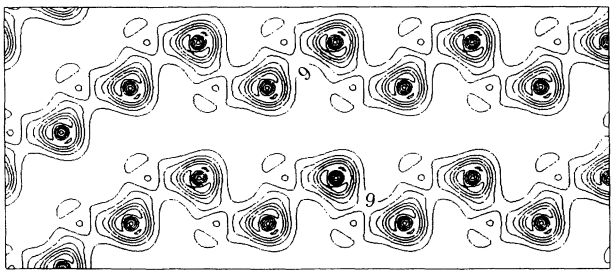

FIG. 4. Contour plot of the valence charge density of the unrelaxed configuration of Fig. 1, in the plane of the bond chains, normalized to eight electrons per unit cell (i.e., multiplied by a factor of $\frac{1}{9}$). The successive contours are equally spaced and are separated by five electrons per unit cell.

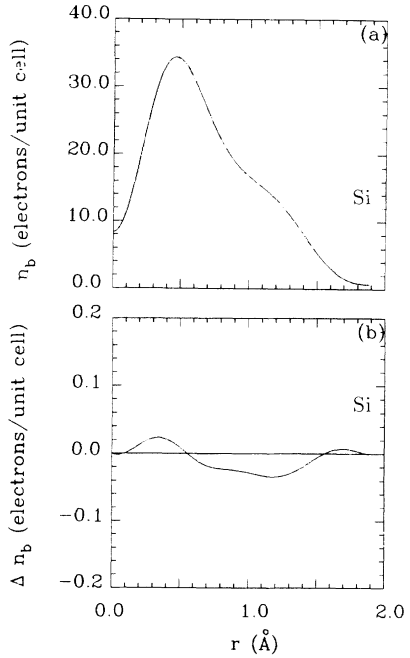

FIG. 5. (a) The valence charge density n_b along bonds 1 and 2 shown in Fig. 1, which are indistinguishable on the scale of the figure. (b) The difference between them, Δn_b, defined as $n_{b,2} - n_{b,1}$.

the T bonds, contrary to what one might think from the relaxation of the $\langle 1 \rangle$ structure of SiC.

Figure 6 may also give some insight about the electric dipole to be expected from an isolated antiphase boundary shown in Fig. 3. Using the arguments of Northrup, Ihm, and Cohen,[16] one can define the interfaces between such a boundary and the surrounding cubic regions (shown in Fig. 3 by dashed lines). The charge-density redistribution in the L bond of the antiphase boundary can be approximated by that of a similar bond in the bulk $\langle 1 \rangle$ structure; this is probably a good approximation since the next two bonds on both sides of this bond are the same in the two structures. Assuming that the charge distribution goes very rapidly to its cubic form away from

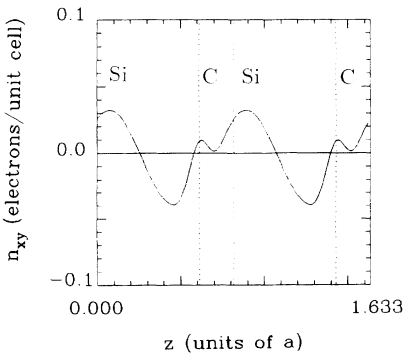

FIG. 6. Difference of the charge density averaged in the planes normal to stacking axis (the x-y plane), $\Delta n_{xy}(z)$, between the bulk wurtzite and cubic structures. The position of the Si and C atoms are shown by vertical dotted lines, and z is given in units of a.

the interfaces, one would be inclinded to think that the dipole due to an isolated antiphase boundary is localized in the region of its L bond. However, this is not true. By denoting the locations of the maximum pile-up of electrons and holes as found in Fig. 6 by $-$ and $+$ signs, respectively, in Fig. 1, one can see that the arrangement shown in the lower chain is in good agreement with the averaged charge-density profile of the supercell and the direction of the net dipole in the $\langle 1 \rangle$ region (from right to left), which shows that the dipole due to a single stacking fault should be across the T bond shown in Fig. 3. This finding is also consistent with the corresponding dipole of ZnS.[17] The barrier height created by such a dipole in SiC is expected to be approximately one-sixth of the barrier height shown in Fig. 1 (0.25 eV), giving 0.04 eV compared with 0.07 obtained in the case of ZnS.[17] This suggests that the SP in ZnS polytypes is comparable with that of SiC polytypes.

One may conclude that a better interface than that of Northrup, Ihm, and Cohen[16] can be defined by the location of the maximum pile-up of electrons and holes at the interface regions, which is consistent with the above discussion about the net dipole created in the $\langle 1 \rangle$ region of the SiC supercell shown in Fig. 1 and that of a single stacking fault. These interfaces are found to be closer to the Si side of the interface L bonds, which can be understood in terms of the asymmetry of the Si-C bond. In Sec. IV we will use the interfaces defined in this manner for the VBO calculations.

We have also performed calculations for the relaxed configuration (see Sec. II). The calculated $P_{\rm int}$ in relaxed $\langle 1 \rangle$ SiC is 4.32×10^{-2} C/m^2, which is about 30% larger than in the unrelaxed configuration. In the case of BeO the increase in the polarization from ionic relaxation was about 300%.[2] The modest increase in the macroscopic polarization due to the ionic relaxation in SiC, compared with that of BeO, reflects the much smaller internal relaxations in SiC [$u_{\rm eq}$ is equal to 0.3755 and 0.3785 in SiC (Ref. 1) and BeO (Ref. 2), respectively, compared with the ideal value 0.3750]. In fact, if we neglect the variation of the total SP (we have used this quantity to facilitate the comparison with the results of Ref. 2) of $\langle 1 \rangle$ SiC, ΔP, with respect to the c/a ratio [which is found to be very small compared with that due to u (Ref. 2)], then we find that $\partial\Delta P/\partial u$ is equal to -2.98 C/m^2, which happens to be close to the value in BeO (-3.0 C/m^2).

IV. RESULTS FOR THE VALENCE-BAND OFFSET

To investigate the VBO at the interface between different SiC polytypes, we have calculated the VBO at the interface between the unrelaxed $\langle \infty \rangle$ and $\langle 1 \rangle$ forms. The additional effect of the structural relaxation is expected to be small. Since the band gap of SiC varies almost linearly with the hexagonal character, one can assume a similar variation for the VBO and hence deduce the VBO between any two arbitrary polytypes.

Using the sharp interfaces defined in Sec. III (i.e., the interfaces shown in Fig. 1 by dashed-dotted lines), the calculated potential lineup is found to be very small, about 0.02 eV. On going from the cubic $\langle \infty \rangle$ to the $\langle 1 \rangle$ structure, the triplely degenerate state at the top of the valence band (Γ_{15}) is split by the crystal field in the $\langle 1 \rangle$ structure into a doubly degenerate state (Γ_5) and a singlet state (Γ_1), with the Γ_5 state being higher in energy.[22] The difference in energy between the Γ_5 state of bulk $\langle 1 \rangle$ and the Γ_{15} of bulk $\langle \infty \rangle$ SiC, calculated relative to a common averaged total potential ($\bar{V}_{\rm tot}=0$), is 0.15 eV. This gives a VBO of 0.13 eV between these two states at the interface between the $\langle 1 \rangle$ and $\langle \infty \rangle$ structures, with the Γ_5 state of the $\langle 1 \rangle$ form being higher in energy. Bearing in mind that the difference between the band gaps of the two structures is 0.90 eV, we conclude that a very high percentage (86%) of the band-gap difference is accommodated by a large conduction-band offset. Thus, our calculations provide a justification for the approximation of zero valence-band offset used in Ref. 11 to discuss the relative stabilities of the various polytypes in the presence of donor and acceptor impurities. Moreover, the crystal-field splitting in $\langle 1 \rangle$ SiC is found to be quite large, 0.12 eV, compared with that of other $\langle 1 \rangle$ materials.[22]

As a result of the SP, an interesting situation may arise when the polarized slab is thick enough such that the potential difference between its two ends is larger than the band gap of the cubic form. To reduce the potential difference a transfer of electrons from the high-potential end to the low-potential one will take place, by creating interface states. These interface states are expected to be quite localized and so they will not affect the linear variation of $\bar{V}_{\rm tot}$ far from the interface. Therefore, even in this situation, both the SP and the VBO are well defined and equal to the values obtained above, provided that the appropriate interface just introduced is used for the latter.

V. INTRINSIC POLARIZATION AND PHASE STABILITY

As pointed out in Sec. I, it is clear from Fig. 1 that the intrinsic dipole moments in any polytype of SiC except $\langle \infty \rangle$ lead to substantial internal electric fields. We need to discuss more critically whether these fields contribute to the energy of the polytypes, in addition to what has already been taken into account in earlier work.[4–8] There are two situations to consider, firstly the polytype without free carriers, and secondly a long period polytype with some free carriers being present at the temperature of crystal growth. In the latter case the carriers can lower their energy by responding to the voltage variations analogous to that in Fig. 1, thus screening the field. As we shall see, in both cases everything has already been included in the existing calculations.[4–8]

We start with some elementary considerations of electrostatics for which no suitable reference could be found. Consider the simple polytype $\langle 3 \rangle$ with a SP around each antiphase boundary. The electrostatic potential in a finite slab with free surfaces would be as shown in Fig. 7(a), where for simplicity we have idealized the potential rise at the dipole layer as a sharp step. However, this would give an enormous voltage difference between the two surfaces of the slab. In reality this macroscopic voltage

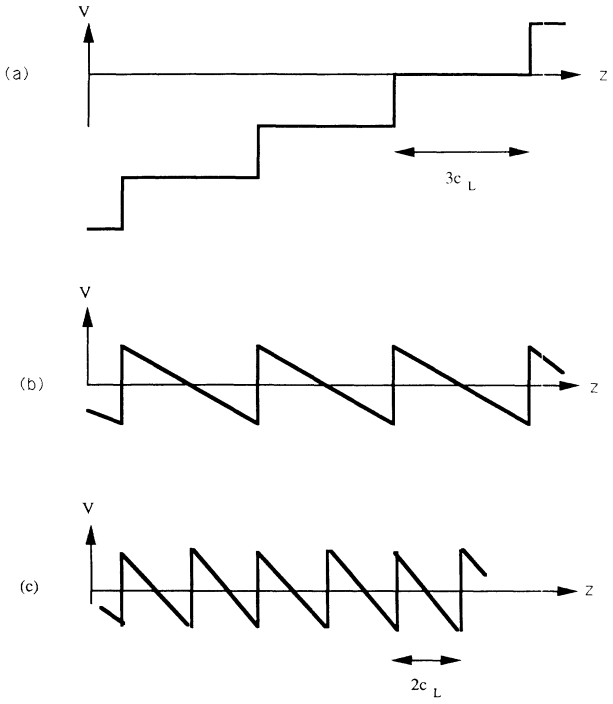

FIG. 7. Averaged potential $\bar{V}(z)$ in simple polytypes (schematic). (a) $\bar{V}(z)$ in $\langle 3 \rangle$ as it would be for a finite crystal with free surfaces and no screening. (b) The same after screening, or in a calculation with periodic boundary conditions. (c) The same as (b) but for polytype $\langle 2 \rangle$.

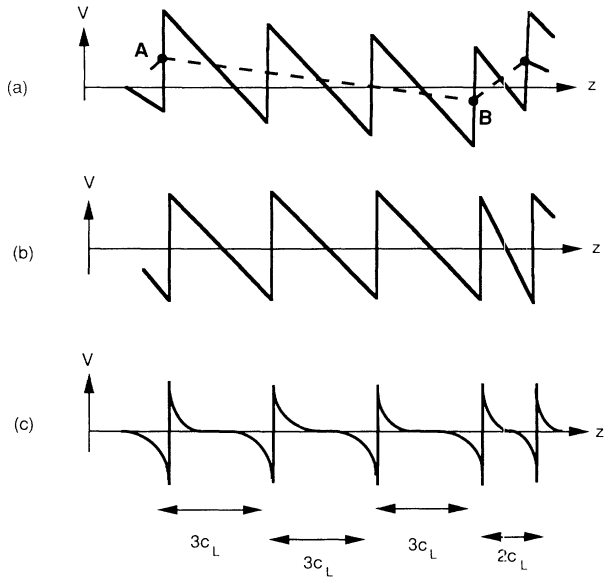

FIG. 8. Periodic averaged potential $\bar{V}(z)$ in one unit cell of the polytype $\langle 3332 \rangle$ (schematic). The sharpness of the rise due to the intrinsic dipole moments at the antiphase boundaries is exaggerated, as is the length ratio of the 3-bands and 2-bands. (a) $\bar{V}(z)$ with very-long-range screening only. Note the Fourier component of $\bar{V}(z)$ with wavelength $11c_L$, and the identical slopes (electric field) in the 2- and 3-bands. (b) $\bar{V}(z)$ with the potential in each 3-band and 2-band as it would be in the polytypes $\langle 3 \rangle$ and $\langle 2 \rangle$. (c) The same as (b) but with a smaller screening length.

would be screened out by ions attracted to the surface from the air, and/or in SiC by the polarization of donors and/or acceptors including the motion of free carriers at the high temperature of crystallization. The resulting voltage variations would therefore be those of Figs. 7(b) and 7(c) of polytypes $\langle 3 \rangle$ and $\langle 2 \rangle$, respectively. The reduction in the energy turns out to be

$$\frac{-P_s^2}{2\epsilon_0 n c_L} \tag{6}$$

per 2-band or 3-band of length nc_L (where c_L is the length of one layer, equal to $c/2$) and per unit area parallel to the layers, where P_s is the dipole moment per unit area of the antiphase boundary. This energy turns out to be comparable to the energy differences between polytypes,[4-8] and we believe it must be included in a proper definition of the bulk energy.

Calculations of polytype energies[4-8] employ periodic boundary conditions, so that the potentials look like those in Figs. 7(b) and 7(c). The energy calculations include correctly the electrostatic contribution and thus implicitly include the correction term Eq. (6). We conclude that they correctly represent the bulk energies of the polytypes without further additions, at least for the simple polytypes $\langle 1 \rangle$, $\langle 2 \rangle$, and $\langle 3 \rangle$.

The situation is a little more complicated for a polytype of longer period such as $\langle 3332 \rangle$ shown in Fig. 8. Subtracting to the constant macroscopic field for a finite slab or performing a calculation with periodic boundary conditions would give a potential as shown in Fig. 8(a). Note that this still leaves a long-wavelength variation in the potential shown by the dashed line in Fig. 8(a) with a maximum variation of about 13 meV (using the results of Sec. III) from A to B. We presume that mobile carriers would be sufficiently localized to take advantage of this variation in the potential and move from around A to around B, with a further drop in the total energy.

At one time we thought this process gave an extra stabilization of the long-period polytypes. However, the screening of the dashed potential in Fig 8(a) is not the correct approach to the point at issue. In previous work[4-8] on the complex polytypes made up of 3-bands and 2-bands (i.e., sections from the structures $\langle 3 \rangle$ and $\langle 2 \rangle$), we took as our zeroth-order model the reference energy which simply adds up the energies of the relevant number of 3-bands (E_3) and 2-bands (E_2), i.e.,

$$E(\text{per unit cell}) = 3E_3 + E_2 \tag{7}$$

for the polytype $\langle 3332 \rangle$ of Fig. 8. This means that the energy given by Eq. (7) corresponds to the potential variation of Fig. 8(b) which is exactly what would result from screening out the long-wavelength part of the potential in Fig. 8(a). The energy lowering from the latter type of screening is therefore already included in the zeroth-order model [Eq. (7)] and therefore no further stabilization of the long period polytypes is produced in this way.

Finally, we need to elaborate on some implicit assump-

tions about the screening, which can best be expressed in terms of the screening length λ_{sc}. In going from Fig. 8(a) to Fig. 8(b) or 8(c) we assumed λ_{sc} to be less than the macroscopic thickness of the finite slab, but longer than $3c_L$ (and $2c_L$). In the discussion of Figs. 8(a) and 8(b) λ_{sc} was assumed to be less than $11c_L$, or whatever the repeat length of the complex polytype is. This is probably a reasonable assumption from what one knows about the localization of carriers in quantum-well structures and the voltage amplitude of the 13 meV already mentioned. Figure 8(c) shows the potentials if λ_{sc} becomes less than $2c_L$, here of order c_L. This is not considered realistic but Fig. 8(c) makes the point that any λ_{sc} much less than $11c_L$ does not affect the argument of Eq. (7): the potential in Fig. 8(c) is manifestly made up of screened 3-band and screened 2-band potentials such as they would appear in pure polytypes $\langle 3 \rangle$ and $\langle 2 \rangle$. Of course these arguments are not exact if λ_{sc} is comparable to $11c_L$.

VI. SUMMARY

Using a first-principles pseudopotential technique and the local-density approximation of density-functional theory for the exchange-correlation potential, we have studied the spontaneous polarization (SP) in wurtzite-structure $\langle 1 \rangle$ SiC and the valence-band offset (VBO) at the interface between the $\langle \infty \rangle$ and $\langle 1 \rangle$ structures. We have also investigated the effect of the resulting macroscopic electric fields on the relative stability of SiC polytypes. In the following we summarize our main results and conclusions.

The SP in $\langle 1 \rangle$ SiC is predicted to be 4.32×10^{-2} C/m^2, and it is mainly due to the electronic charge redistribution. The ionic relaxation is found to have only a small effect, about 25% of the above value is due to this relaxation, contrary to the case of $\langle 1 \rangle$ BeO.[2] This is a consequences of the much smaller internal relaxation in $\langle 1 \rangle$ SiC.[1,2] The SP is expected to vary linearly with the density of stacking faults, which indicates that the SP in other SiC polytypes varies linearly with the degree of hexagonality. Note that the cubic structure has no SP by symmetry.

The electronic charge transfer in unrelaxed $\langle 1 \rangle$ SiC, which causes the SP, is found to be rather complicated. From the difference in the planar-averaged density (averaged normal to the stacking direction) between the unrelaxed $\langle 1 \rangle$ and $\langle \infty \rangle$ forms, we found that most of the charge transfer takes place across the transverse bond regions. Moreover, there is an excess of charge in the transverse bond regions which is consistent with the form of the structural relaxation. This is not evident in the charge density plotted along the bond direction, which in fact shows that the longitudinal bonds have higher charge density along that line: the latter must be outweighted by the longitudinal to transverse bonds electron transfer elsewhere in the three-dimensional region of the bonds.

Our results give some insight into the electric dipole due to an isolated antiphase boundary, which is expected to be localized across the transverse bond of the antiphase boundary and gives a barrier height of around 0.04 eV.

The VBO at the interfaces between SiC polytypes turn out to be rather small, with a maximum value of 0.13 eV between the extreme cases of the $\langle 1 \rangle$ and $\langle \infty \rangle$ structures. Thus almost the whole of the large difference in the band gaps between these materials appears as a conduction-band offset. Since the band gap varies nearly linearly with the degree of hexagonality of the structures, we expect the same behavior, suitably scaled, to apply to the VBO between any two polytypes. This confirms the argument[11] that acceptor impurities should contribute very little to the relative phase stability of the $\langle 1 \rangle$ and $\langle \infty \rangle$ forms, but that donors should favor significantly the one with the smaller band gap.[11] The crystal-field splitting of the top of the valence band is found to be 0.12 eV in $\langle 1 \rangle$ SiC.

We have considered two electrostatic effects arising from the intrinsic dipole moments, and the screening of the resulting electric fields. In neither case have we found any identifiable contribution to the relative phase stability of polytypes.

Recently we performed self-consistent pseudopotential calculations for the disturbance of the charge density around an isolated tacking boundary in SiC polytypes.[23] In light of these additional calculations we were able, among other things, to extract direct information about the location, direction, and localization of the electric dipole due to an isolated stacking fault. These results were found to be in good agreement with the predictions made in this paper, which supports our choice of the interface. Moreover, we have found that the SP varies linearly with the degree of the hexagonality, as has been assumed in this paper.

ACKNOWLEDGMENTS

The authors are grateful to R. Resta and M. Posternak for illuminating discussions, and the Science and Engineering Research Council (U.K.) for financial support.

*Present address: Center for Theoretical and Applied Physics, Yarmouk University, Irbid, Jordan.

[1] C. Cheng, V. Heine, and R. J. Needs, J. Phys. Condens. Matter **2**, 5115 (1990).

[2] M. Posternak, A. Baldereschi, A. Catellani, and R. Resta, Phys. Rev. Lett. **64**, 1777 (1990); M. Posternak, R. Resta, and A. Baldereschi (unpublished).

[3] C. J. Schneer, Acta Crystallogr. **8**, 279 (1955).

[4] C. Cheng, R. J. Needs, and V. Heine, J. Phys. C **21**, 1049 (1988).

[5] C. Cheng, V. Heine, and R. J. Needs, Europhys. Lett. **12**, 69 (1990).

[6] C. Cheng, V. Heine, and I. L. Jones, J. Phys. Condens. Matter **2**, 5097 (1990).

[7]C. Cheng, R. J. Needs, V. Heine, and I. L. Jones, Phase Transitions **15**, 311 (1989).

[8]V. Heine and C. Cheng, in *Geometry and Thermodynamics: Common Problems of Quasi-Crystals, Liquid Crystals and Incommensurate Insulators,* edited by J. C. Tolédano (Plenum, New York, 1990).

[9]S. B. Austerman, D. A. Berlincour, and H. H. A. Krueger, J. Appl. Phys. **34**, 339 (1963); E. Loh, Phys. Rev. **166**, 673 (1968); *Elastic, Piezoelectric and Related Constants of Crystals,* edited by O. Madelung, Landolt-Börnstein, Vol. III (Springer-Verlag, Berlin, 1979), Chap. 11.

[10]K. J. Chang, S. Froyen, and M. L. Cohen, Phys. Rev. B **28**, 4736 (1983), and references therein.

[11]V. Heine, C. Cheng, and R. J. Needs (unpublished).

[12]R. M. Martin, Phys. Rev. B **9**, 1998 (1974).

[13]A. Baldereschi, S. Baroni, and R. Resta, Phys. Rev. Lett. **61**, 734 (1988).

[14]*Numerical Data and Functional Relationships in Science and Technology,* edited by O. Madelung, Landolt-Börnstein, Vol. 17a (Springer, New York, 1981).

[15]A. Qteish and R. J. Needs, Phys. Rev. B **42**, 3044 (1990).

[16]J. E. Northrup, J Ihm, and M. L. Cohen, Phys. Rev. B **22**, 2060 (1980).

[17]J. E. Northrup and M. L. Cohen, Phys. Rev. B **23**, 2563 (1981).

[18]*Theory of the Inhomogeneous Electron Gas,* edited by S. Lundqvist and N. H. March (Plenum, New York, 1983).

[19]D. M. Ceperley and B. J. Alder, Phys. Rev. Lett. **45**, 566 (1980).

[20]J. Perdew and A. Zunger, Phys. Rev. B **23**, 5048 (1981).

[21]H. J. Nonkhorst and J. D. Pack, Phys. Rev. B **13**, 5188 (1976).

[22]J. O. Dimmock, in *II-VI Semiconductor Compounds, 1967 International Conference,* edited by D. G. Thomas (Benjamin, New York, 1967), p. 277.

[23]A. Qteish, V. Heine, and R. J. Needs (unpublished).